Rev.Adv.Mater.Sci. 8 (2004) 1-9

EPITAXIAL Ag NANOWIRES ON Si(111) GENERATED VIA ELECTRON BEAM LITHOGRAPHY IN ULTRAHIGH VACUUM

V. Zielasek, T. Block and H. Pfnür

Institut für Festkörperphysik, Universität Hannover, Appelstr. 2, D-30167 Hannover, Germany

Received: October 26, 2004

Abstract. Electron beam lithography in ultra-high vacuum is combined with epitaxy of silver on Si(111) to generate crystalline metal nanowires of few atomic layers thickness and a width of less than 20 nm on an insulating support. The experiments are performed in a combined SEM-STM system for confocal and simultaneous operation of both microscopes at variable sample temperatures in the range 60-900K. Employing electron beam-induced selective thermal desorption, clean Si(111) windows are generated within a thin thermal surface oxide layer of 0.3-0.7 nm thickness. During deposition of Ag at a sample temperature of 130K small Ag islands nucleate in the Si windows as well as on the oxide areas. Subsequent annealing to room temperature or above leads to the formation of continuous flat epitaxial Ag islands constricted to the window areas. When the surface is annealed up to 700K the islands coalesce in the direction that is unconstricted by the oxide mask up to a length of some 100 nm while spherical non-percolated Ag clusters with diameters of several nanometers form on the oxide areas.

1. INTRODUCTION

Metal nanostructures have interesting prospects for future nanoelectronics applications. Compared to semiconductors, metals feature a high density of charge carriers for electrical transport so that metal nanowires may be benefitial when single molecules or components of molecular electronics need to be contacted on a scale of few nanometers. With characteristic dimensions and electron confinement in the range of the Fermi wavelength, metal nanostructures are also expected to reveal interesting quantum phenomena which may be exploited for nanoscale devices. Metal-based single-electron transistors have been demonstrated to work up to room temperature [1] because the energy difference of quantum levels is increasing as the scale of confinement is getting smaller.

With metal nanostructure cross sections on the scale of few atomic distances single structural defects become important for the electronic properties. Therefore the nanostructures should be well-defined on the atomic scale, meaning that they should be crystalline and exhibit either no defects or the defects should be at least well characterized. Furthermore, the metal nanostructures should be generated on an insulating support so that arbitrary lateral shapes and circuits may be formed.

Bottom-up approaches to the generation of atomically well-defined metal nanostructures usually exploit self-organisation during metal epitaxy and have demonstrated the generation of more or less perfect atomic chains or wires [2]. These structures, however, have been generated mostly on specific metal substrates and their shape is determined by the morphology of the underlying substrate. On the other hand, top - down approaches that employ high-resolution electron beam-, X-ray-, or ultraviolet lithography render possible the generation of nanoscale metal structures of arbitrary lateral shape also on insulating substrates. Here, however, the structures usually exhibit a lot of defects because the metal does not form epitaxial layers on the chosen sub-

Corresponding author: V. Zielasek, e-mail: zielasek@fkp.uni-hannover.de

© 2004 Advanced Study Center Co. Ltd.

strate and *ex situ* processes involving organic photoresists and etches cause contamination. So far epitaxial metal nanostructures with characteristic dimensions in the range of some 10 nm on insulating substrates have been reported for Mo on sapphire [3].

Here we report on our first results of combining electron beam lithography with epitaxy of silver on silicon for the generation of epitaxial metal nanowires on an insulating support. In order to avoid surface contamination induced by lithographical processes we employ an *in situ* nanolithography technique for silicon surfaces developed by M. Ichikawa and his group that takes place in ultra-high vacuum, entirely. It will be demonstrated that this nanolithography technique in combination with low-temperature silver epitaxy may generate ultrathin continuous epitaxial metal nanowires with a width below 20 nm.

2. EXPERIMENTAL

The experiments were carried out in ultrahigh vacuum (base pressure below $3 \cdot 10^{-8}$ Pa) in a combined scanning electron microscope (SEM) – scanning tunneling microscope (STM) system (JEOL SPM 4500 SX). Both microscopes are confocal and can be operated simultaneously at variable sample temperatures in the range 60-900K. While the electron gun (1-25 keV) provides an SEM resolution of 4 nm, an eucentric tilting mechanism of the sample stage renders possible to vary the angle of incidence of the electron beam between 0 and 30° (see Fig. 1). At glanzing incidence microprobe reflection high-energy electron diffraction (μRHEED) may be used to check the crystillanity of generated structures. By means of a movable optical detector underneath the RHEED screen the intensity of any diffraction spot may be chosen as input signal for scanning reflection electron micrographs (SREM). The system is additionally equipped with an electron energy analyzer that enables us to perform Auger electron spectrocopy (AES) and scanning Auger electron microscopy (SAM).

The Si(111) substrate samples, sized 0.3x1.5x7 mm, were cut from wafers of high resistivity (>1000 Ωcm). The substrate surfaces were prepared by repeated flash-heating to 1400K by direct current while keeping the ambient pressure below $1 \cdot 10^{-7}$ Pa. To oxidize the surface the sample temperature was raised to 943K for 10 min after oxygen (99.999%) was introduced into the chamber at a pressure of $2 \cdot 10^{-4}$ Pa. It has been demonstrated before that a complete layer of oxide, 0.3 nm thick, is formed under these conditions [4-6]. The surface quality

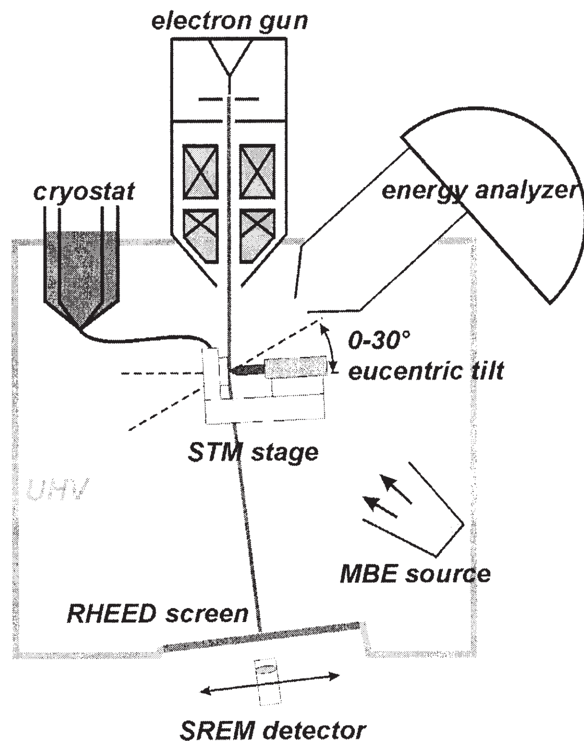

Fig. 1. Schematic of the SEM-STM main chamber set up for SAM, RHEED, and SREM. Sample (facing to the right) and STM are mounted on a stage for eucentric tilting with respect to the SEM. Sample temperature can be varied in the range 60–900K during microscopy.

and contamination was monitored by STM, RHEED, and AES. Silver was evaporated from a well-outgassed Knudsen cell. The deposition rate was determined using a quartz microbalance calibrated via STM measurements. For calibration Ag was deposited in submolayer amounts onto the substrate held at a temperature of 700K. The areal fraction of Si(111) ($\sqrt{3}$ x $\sqrt{3}$)-Ag regions was determined and the Ag coverage calculated, assuming a density of 1 Ag atom per Si atom of the topmost layer ($7.83 \cdot 10^{14}$ cm^{-2}) in the ($\sqrt{3}$ x $\sqrt{3}$)-reconstructed regions according to the HCT model [7].

3. RESULTS

The lithographical process is shown schematically in Fig. 2. After preparation of a clean Si(111)-(7x7) substrate surface a complete ultrathin thermal surface oxide layer is generated. Selected areas are irradiated by the focused electron beam, stimulat-

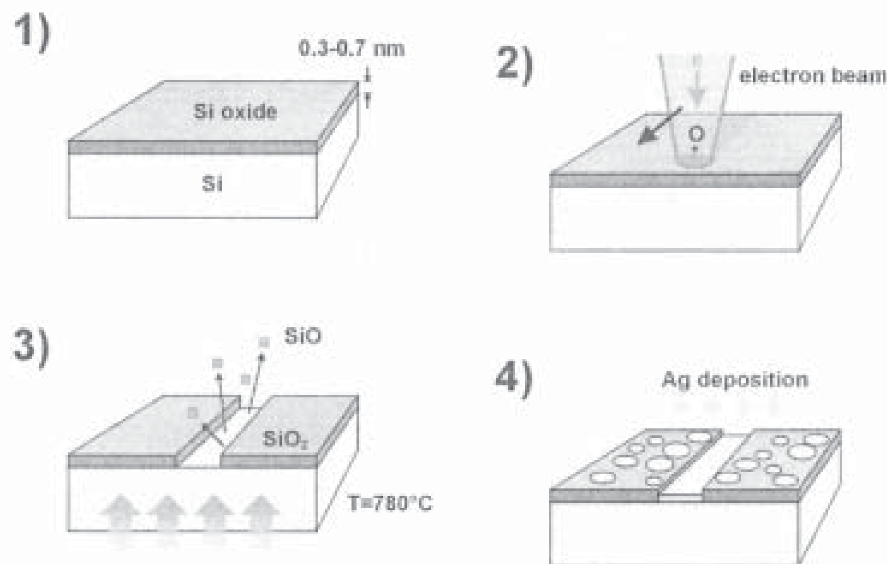

Fig. 2. Schematic of e-beam lithography in UHV for the generation of silver nanostructures on silicon: thin thermal oxide on Si (1), electron-induced oxygen desorption in selected areas (2), void formation in the oxide via thermal desorption of SiO (3), and Ag deposition leading to cluster formation in oxide areas and epitaxial Ag layers in Si window.

ing desorption of oxygen from the oxide. The surface is then heated so that SiO desorbes from the irradiated areas while SiO_2 remains stable on the surface, thereby leading to the formation of Si windows with sharp boundaries to the surrounding oxide. Silver is then deposited at low temperature on the surface and annealed, forming clusters on the oxide areas and epitaxial layers in the Si windows.

The following presentation of first results is arranged according to our experimental approach and starts with the generation of Si windows within a thin thermal oxide. Then details of the epitaxy of silver on bare Si(111) and on Si(111)/Si oxide templates will be reported while a third subsection on the Ag wetting layer completes the results.

3.1. Generation of Si(111)/Si oxide templates

The formation of clean silicon windows in an oxide mask due to electron-beam induced selective thermal decomposition and desorption of the oxide has been described in detail by M. Ichikawa and coworkers [8,9]. The width of the silicon windows depends on the primary electron dose and the duration of the subsequent heating. The total electron dose has to be optimized in order to obtain continuous Si windows while maintaining a good lateral resolution as the plume of secondary electrons damages the oxide around the focus of the primary electron beam. In our experiments the sample surface was irradiated at an angle of ≈10° with respect to the surface plane with a total surface electron dose of 100-200 C/cm^2 and an electron energy of 25 keV. After electron irradiation the surface was heated up to 780 °C for 10-30 s. Besides the desorption of SiO, etching of SiO_2 by bared Si leads to the decomposition of the oxide [6] which is seen by a continuous propagation of the oxide boundary and widening of the Si windows during prolonged heating. STM has demonstrated that the Si surface in the window areas is atomically clean.

Fig. 3 shows a ring-shaped Si(111) window within an oxide mask as seen by SEM, SREM, and STM. The visibility of the generated structures by SEM or SREM is a prerequisite for navigating the STM tip towards the area of interest. The SREM image was generated using the intensity of a first order RHEED spot on the fluorescent screen as input sgnal for the scanning electron micrograph. The Si window appears as bright area due to the high lateral order of the clean Si(111) surface. On the contrary the secondary electron emission exhibits only weak contrast between the oxide and the window areas. Only the boundary between the thin oxide layer and the bared substrate area is visible as bright feature in the SEM image, probably due to topographic contrast.

Fig. 4 shows line-shaped Si(111) windows which were generated as templates for silver nanowires. With electron doses and the subsequent heating procedure optimized, the windows are continuous over a distance of several micrometers (Fig 4a). We

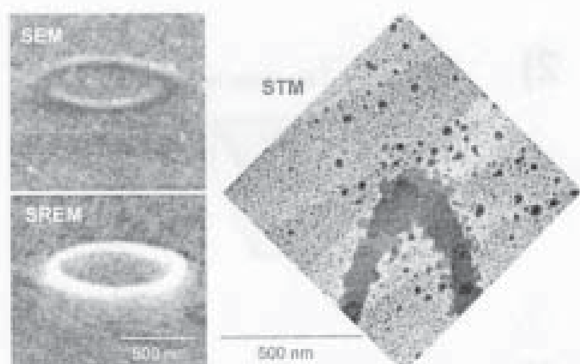

Fig. 3. Ring-shaped Si(111) window in oxide mask: SEM shows border between oxide and window area while SREM (integer-order RHEED spot intensity as input signal) shows well-ordered Si(111) surface in window area. Right panel: STM of widest section of ring-shaped window. The width is due to the small angle of incidence (≈10° with respect to the surface plane) during lithography.

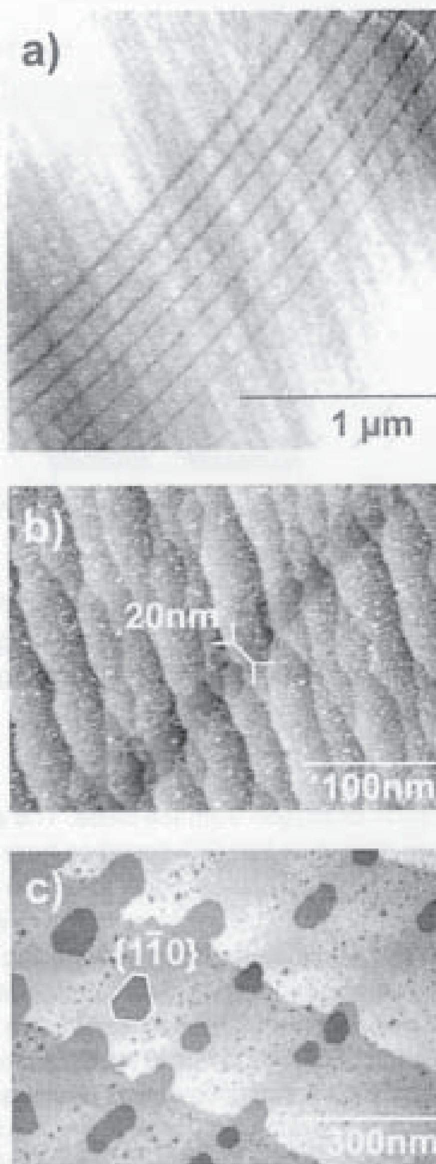

Fig. 4. STM: (a) Line-shaped Si(111) windows in Si oxide mask generated by electron irradiation (total doses 30-300 C/cm^2). (b) Detail of lineshaped Si(111) window with a width of 20 nm. (c) Etch pits (one atomic layer deep) along {1$\bar{1}$0} directions after prolonged heating.

have generated windows as narrow as 10 nm while windows with a width of 20 nm as shown in (b) are achieved regularly, also on substrates with a high step density where the boundaries between oxide and windows often appear less sharp than on large single terraces. Fig. 4c shows the result of prolonged heating after electron irradiation. The consumption of silicon from the bared areas during decomposition of the oxide is evident by etch pits that form especially at atomic steps but also on flat Si(111) terraces in the window areas. The etch pits are one atomic layer deep and their borders are probably aligned along {110} directions as observed, e.g., for Si(1$\bar{1}\bar{1}$) etching by water [10].

3.2. Ag epitaxy

Having Si(111)/Si oxide templates, the deposition of silver is the next step in the lithographical process. On bare silicon surfaces silver grows epitaxially without forming silicides, making silver an ideal candidate for insulated metal nanostructures on silicon with a well-defined interface between metal and substrate. Before depositing silver on Si/Si oxide templates we have studied the growth of Ag layers on bare Si(111), varying growth parameters in a range that appears promising for the generation of continuous Ag nanowires.

At room temperature silver grows on Si(111) in the Stranski-Krastanov mode [11]. However, for silver deposition at low temperatures (< 170K) and various annealing procedures, a variety of metastable structures have been reported as a result of limited kinetics. STM studies have shown that silver grows layer by layer and is atomically flat at a sample temperature of 100K [12]. Layer by layer growth has also been observed for deposition at 150-170K [13]. With increasing amount of deposited material interconnected islands, flat islands on top of a rough wetting layer, and continuous Ag layers

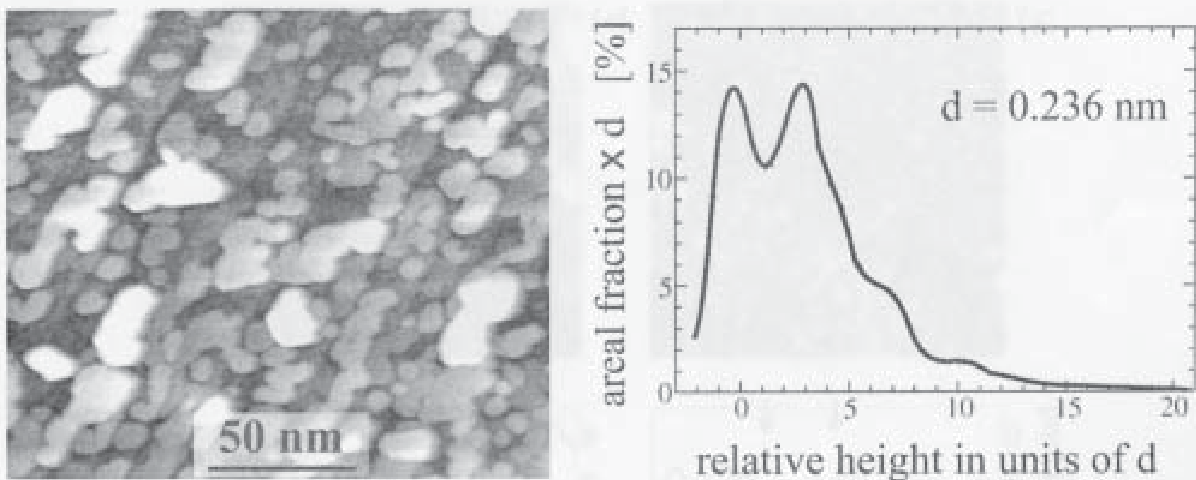

Fig. 5. Left panel: STM of 4 ML Ag/Si(111) deposited at 130K and annealed to room temperature. Right panel: Histogram of relative height in units of d=0.236 nm (thickness of Ag(111) monolayer) showing preferred heights of 3 and 7 d.

have been observed when the surfaces were annealed to room temperature after deposition [14]. For the flat islands preferred island heights have been identified. While the reason for the occurence of different preferred heights in seemingly similar experiments (2 ML [13-15] and 6 ML [16]) has not been clarified, yet, these magic heights are ascribed to a contribution of electron confinement within the metal layer to its free energy [15]. Spot profile analysis of LEED has shown that the continuous films consist of atomically flat grains, forming a small-angle (6°) rotational mosaic [17]. Grain diameters in the range of 1.5 to 9.5 nm have been observed, depending on the substrate temperatures during deposition and annealing.

Fig. 5 shows an STM image of 4 ML Ag on Si(111) with a high step density (average terrace width ≈ 15 nm) deposited at 130K and annealed to room temperature by passing a small direct current through the sample. Atomically flat islands with diameters up to some 10 nm are observed on top of a wetting monolayer which shows corrugation in STM. The islands are aligned along the step edges and exhibit preferred heights as depicted in the histogram shown in the right panel of Fig. 5. The features of the height distribution are very wide because the relative height was determined with respect to a reference plane, neglecting the substrate steps and the inclination of the substrate terraces with respect to the reference plane. Nevertheless magic heights of 3, 7, and 10 monolayers above the wetting layer can be observed. Comparing our result to previously reported magic heights of 2 and 6 ML above the wetting layer, respectively, we may only speculate that the preferred island thickness is altered in presence of substrate steps.

Fig. 6 shows an STM image of 10 ML Ag on a Si(111) substrate with a low step density and wide terraces in the range of 100 nm. The silver layer was deposited at 130K and annealed to room temperature. Instead of a continuous Ag layer we find a percolated network of islands, obviously aligned

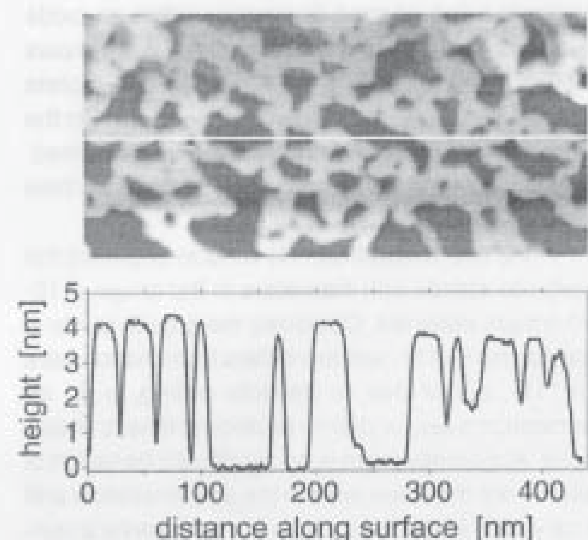

Fig. 6. STM of 10 ML Ag/Si(111) deposited at 130K and annealed to room temperature showing percolated network of flat islands. Line scan shows narrow range of island height around 4 nm.

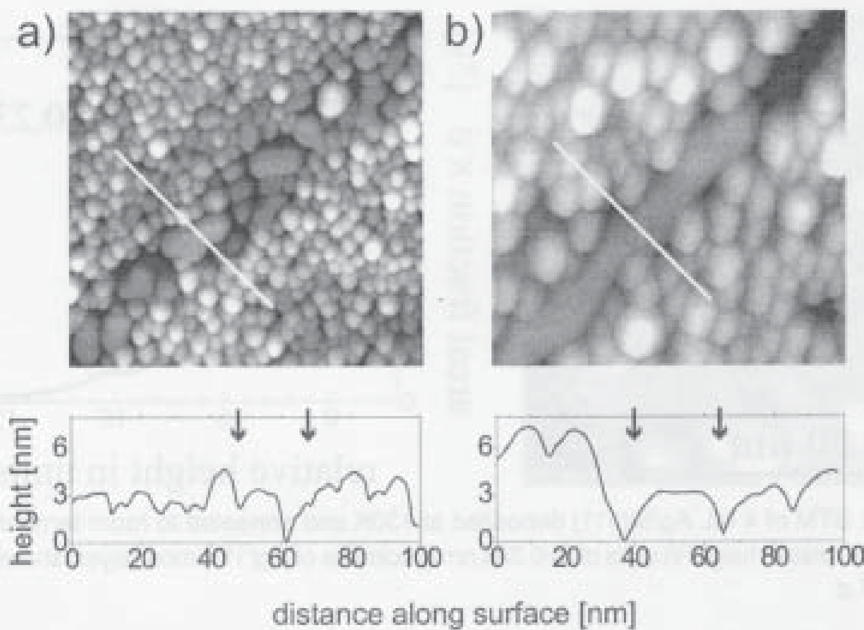

Fig. 7 STM (150x150 nm^2, sample bias +8 V, tunneling current 45 pA) of 7 ML Ag deposited at 130K on line-shaped Si(111) window in oxide mask and annealed to (a) 300K and (b) to 700K, respectively. Height profiles under the STM images show 3 nm high Ag islands in window areas (borders of window areas are marked by arrows). The positions of the height profiles are depicted as white lines within the corresponding STM image.

along low-index directions of the substrate lattice (the STM image in Fig. 6 is not corrected for thermal drift). The islands have all about the same height of 4 nm with a variation of not more than ±15%, as the line scan in Fig. 6 shows.

Such a percolated network of islands of uniform height in a line-shaped Si window within an oxide mask would make a perfect nanowire. Fig. 7a shows 7 ML Ag deposited on a Si(111)/Si oxide template at 130K and annealed to room temperature. On the oxide area spherical Ag nanoclusters have formed. The low surface free energy of the oxide surface inhibits a metal wetting layer.

In the line-shaped Si(111) window separate flat epitaxial islands with diameters in the range of 10-20 nm are detected. Obviously the growth mode in the narrow Si(111) window differs from that on bare Si(111), either due to defects acting, e.g., as nucleation sites, or due to additional kinetic limitations. Apparently there is no significant transport of silver from the oxide area to the silicon window and vice versa. All material hitting the oxide area is consumed by the clusters. When diffusional transport of silver atoms is restricted to the line-shaped Si(111) window, any coarsening of islands may be hindered.

The STM measurements on Ag-covered oxide areas require rather high sample biases and low currents in order to keep the distance between tip and surface large enough so that picking-up and moving-around silver atoms from the surface is avoided. The STM images in Fig. 7 have been taken with a sample bias of +8 V and at a tunneling current of 50 pA, compromising tip stability with resolution.

Fig. 7b shows the result of annealing 7 ML Ag deposited at 130K on a line-shaped Si(111)/Si oxide template up to about 700K. Comparison with (a) reveals that the clusters on the oxide have coarsened. Still they appear to be spherical in shape, indicating that they are not interconnected. Within the Si(111) window a single elongated island has formed. The line scan depicted underneath the STM image reveals that the island is about 3 nm high, has a flat top, and is separated from the adjacent clusters on the oxide area.

Such nanowire sections have been observed with a total length up to 250 nm in our STM experiments. Fig. 8 shows two nanowire sections with a width of 15-25 nm in adjacent Si(111) windows. The disturbances visible in the STM image are due to tip changes, presumably induced by detachment or at-

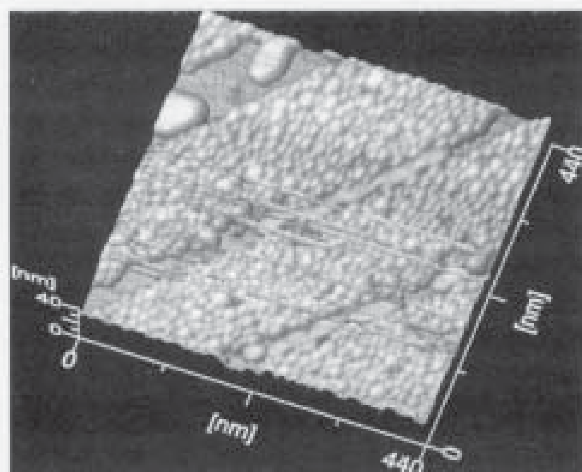

Fig. 8. STM of Ag deposited on Si(111)/Si oxide template showing wire-shaped metal islands in narrow Si windows (width of 20 nm) and 2D islands in wider window (80 nm).

tachment of silver atoms. Fig. 8 also shows two islands in an 80 nm wide Si(111) window. Their lateral shape appears as round as it is expected for silver deposition on bare silicon. Obviously, the tendency to form elongated nanowire sections is promoted by narrow Si windows. The role of the interface between the Si window and the oxide for Ag diffusion and nucleation of Ag islands has not been investigated, yet.

3.3. Ag wetting layer

When silver on Si(111) is annealed up to 700K or deposited at that temperature, a wetting monolayer forms which is composed of ($\sqrt{3} \times \sqrt{3}$)-Ag domains [18]. The ($\sqrt{3} \times \sqrt{3}$)-Ag surface has a metallic surface state band as demonstrated by the observation of standing electron waves [19] and a two-dimensional plasmon [20]. Furthermore, a surface state conductivity in the range of $5\text{-}10 \cdot 10^{-5}\ \Omega^{-1}$ has been reported [21]. Consequently, besides the 3 nm high nanowire sections, the Ag wetting layer in the Si(111) windows may be regarded as a metal nanowire in its own right. In contrast to the nanowire sections the wetting layer is limited in length only by the size of the Si(111) window.

The wetting layer formation on bare Si(111) is shown by STM in Fig. 9a. An amount of 0.25 ML Ag was deposited at a temperature of 700K and at a deposition rate of 0.05 ML/min. Continuous areas of ($\sqrt{3} \times \sqrt{3}$)-Ag domains decorate the substrate steps. The adatoms of the clean Si(111) (7x7) re-

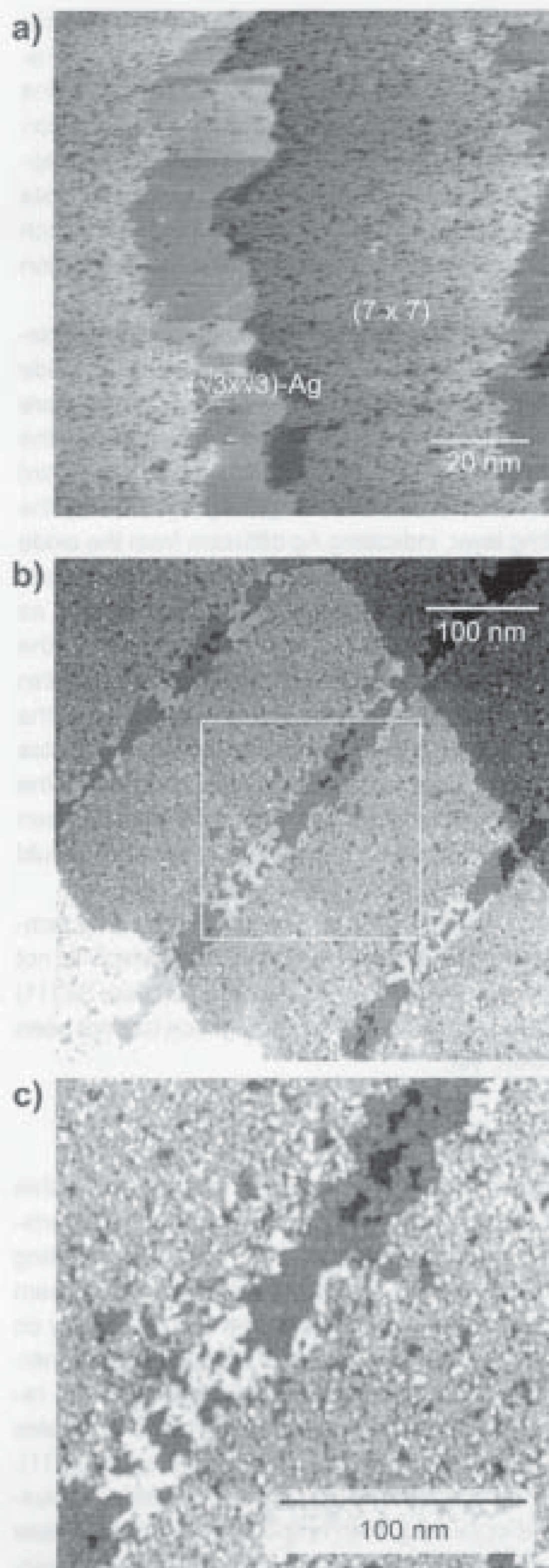

Fig. 9. STM images: (a) 0.25 ML Ag deposited on Si(111) at 700K at a rate of 0.05 ML/min. Decoration of steps by ($\sqrt{3} \times \sqrt{3}$)-Ag islands. STM shows the adatoms of the clean Si(111)-(7x7) area. (b) and (c) 0.5 ML Ag deposited on Si(111)/Si oxide template at 790K at a rate of 0.13 ML/min. Si windows are covered by continuous Ag wetting layer. (c) shows detail of (b).

gions are resolved in the STM image while the atomic details of the ($\sqrt{3}$ x$\sqrt{3}$)-Ag structure are not resolved. Close to the raised ($\sqrt{3}$ x$\sqrt{3}$)-Ag domains at the upper substrate step edge dark regions can be seen within the (7x7) terrace. These regions represent ($\sqrt{3}$ x$\sqrt{3}$)-Ag domains on a lower substrate terrace which form due to the transport of silicon involved in the Ag-induced surface reconstruction [18].

Figs. 9b and 9c show the wetting layer formation in line-shaped Si(111) windows within an oxide mask with panel (c) showing a section of (b) in more detail. While only 0.5 ML Ag were deposited on the surface (dep. temperature: 790K, rate: 0.13 ML/min) the window areas are completely covered by the wetting layer, indicating Ag diffusion from the oxide to the window area. The aforementioned pits due to the Ag-induced surface reconstruction as well as islands of an additional layer can be seen in the window areas. The observed height differences within the windows always correspond to multiples of the Si(111) bilayer thickness. This observation indicates that the Si substrate is completely covered by the wetting layer because the height difference between (7x7) and adjacent ($\sqrt{3}$ x$\sqrt{3}$)-Ag terraces would clearly differ from the Si bilayer thickness.

The wetting layer on the Si(111)/Si oxide templates shows a surface corrugation which is not present on the ($\sqrt{3}$ x$\sqrt{3}$)-Ag areas on bare Si(111) (panel a). The origin of the corrugation has not been clarified, yet.

4. CONCLUSIONS

We have demonstrated the generation of ultrathin crystalline metal nanostructures with characteristic lateral dimensions of 20 nm on an insulating support by means of a combination of electron beam lithography in ultra-high vacuum and Ag epitaxy on Si(111). Line-shaped clean Si windows were generated within a thin thermal oxide layer and the results of silver epitaxy on such Si/Si oxide templates were compared with silver epitaxy on bare Si(111). On the oxide area the formation of spherical Ag clusters is observed. With respect to the bare Si areas the growth modes are similar for both types of substrate. However, we find details of the morphology of the metal deposit depending on the lateral constriction imposed by the oxide mask. Consequently, growth parameters have to be optimized for Si/Si oxide templates individually. So far we have generated two different instances of nanowires: Depositing 7 ML silver at 130K and annealing to 700K we find islands elongated up to few 100 nm and a few nanometer high in narrow (20 nm) Si windows. By depositing submonolayer amounts of silver at a temperature of 790K a continuous wetting layer forms in the window areas. A more detailed analysis of the nanowire morphologies and charactization of their structural details is in progress as we aim at studying the influence of single defects on electrical transport at a later stage.

ACKNOWLEDGEMENTS

V.Z. gratefully acknowledges valuable support and SEM-STM training by M. Ichikawa and A.A. Shklyaev. Financial support has been provided by the Centre for Nanoelectronics of the University of Hannover and by Deutsche Forschungsgemeinschaft.

REFERENCES

[1] Y. Pashkin, Y. Nakamura and J. Tsai // *Appl. Phys. Lett.* **76** (2000) 2256.
[2] H. Brune // Surf. Sci. Rep. **31** (1998) 121.
[3] G. Mikhailov, L. Aparshina, A. Chernykh, S. Dubonos, Y. Koval and I. Malikov // *Nanotechnology* **9** (1998) 1.
[4] H. Watanabe, K. Kato, T. Uda, K. Fujita, M. Ichikawa, T. Kawamura and K. Terakura // *Phys. Rev. Lett.* **80** (1998) 345.
[5] T. Matsudo, T. Ohta, T. Yasuda, M. Nishizawa, N. Miyata, S. Yamasaki, A. Shklyaev and M. Ichikawa // *J. Appl. Phys.* **91** (2002) 3637.
[6] N. Miyata, H. Watanabe and M. Ichikawa // *Phys. Rev. Lett.* **84** (2000) 1043.
[7] M. Katayama, R. Williams, M. Kato, E. Nomura and M. Aono // *Phys. Rev. Lett.* **66** (1991) 2762.
[8] S. Maruno, S. Fujita, H. Watanabe and M. Ichikawa // *J. Appl. Phys.* **82** (1997) 639.
[9] S. Fujita, S. Maruno, H. Watanabe and M. Ichikawa // *J. Vac. Sci. Technol. B* **16** (1998) 2817.
[10] G. Pietsch, U. Köhler and M. Henzler // *Chem. Phys. Lett.* **197** (1992) 346.
[11] E. J. van Loenen, M. Iwami, R. Tromp and J. F. van der Veen // *Surf. Sci.* **137** (1984) 1.
[12] G. Meyer and K. Rieder // *Appl. Phys. Lett.* **64** (1994) 3560.
[13] K. Kimberlin, G. Rutter, L. Nagle, K. Roos and M. Tringides // *Surf. Interface Anal.* **35** (2003) 1069.
[14] C.-S. Jiang, H. Yu, C.-K. Shih and P. Ebert // *Surf. Sci.* **518** (2002) 63.

[15] L. Gavioli, K. Kimberlin, M. Tringides, J. Wendelken and Z. Zhang // *Phys. Rev. Lett.* **82** (1999) 129.

[16] L. Huang, S. J. Chey and J. Weaver // *Surf. Sci.* **416** (1998) L1101.

[17] F. Moresco, M. Rocca, T. Hildebrandt and M. Henzler // *Surf. Sci.* **463** (2000) 22.

[18] K. Wan, A. Lin and J. Nogami // *Phys. Rev. B* **47** (1993) 13700.

[19] N. Sato, S. Takeda, T. Nagao and S. Hasegawa // *Phys. Rev. B* **59** (1999) 2035.

[20] T. Nagao, T. Hildebrandt, M. Henzler and S. Hasegawa // *Phys. Rev. Lett.* **86** (2001) 5747.

[21] C.-S. Jiang, S. Hasegawa and S. Ino // *Phys. Rev. B* **54** (1996) 10389.